Ultraviolet Resonance Raman Spectroscopy of Bulk and Microscopic Human Colon Tissue

NADA N. BOUSTANY,* RAMASAMY MANOHARAN, RAMACHANDRA R. DASARI, and MICHAEL S. FELD

George R. Harrisson Spectroscopy Laboratory, Massachusetts Institute of Technology, Cambridge, Massachusetts 02139

A sensitive ultraviolet resonance Raman (UVRR) system, which integrates bulk and microscopic capabilities, is described for use with human tissue. The system incorporates a quasi-continuous tunable laser excitation source in the range 200–300 nm, a liquid nitrogen-cooled charge-coupled device (CCD), a single grating spectrometer, dielectric longpass laser line rejection filters, and cooled specimen holders to minimize bio- and photo-degradation. The system was used on normal human colon tissue, and was compared to our previously used Nd:YAG-based system. Spectra with higher signal-to-noise ratio (S/N) than has previously been achieved, and with less than 5% photobleaching, are presented. The present system outperforms our previous system by improving the S/N in bulk normal colon spectra by a factor of greater than 10. We show for the first time UVRR spectra collected from the various microscopic regions of human colon in a thin section preparation, and the line shapes from the different microscopic morphological components are related to the bulk colon spectra. At 251 nm the epithelial cells and the lamina propria are the major contributors to the UVRR spectrum of bulk colon tissue. Our data suggest that combined bulk and microscopic UVRR spectroscopy of human tissue could provide a valuable tool for bioassay and histochemistry.

Index Headings: **Ultraviolet resonance Raman spectroscopy; Human colon; Quantitative histology.**

INTRODUCTION

Many clinical and biological studies, including the evaluation of disease biopsies and the examination of live cell metabolism in real time, would benefit from an analytical technique that could quantify the biochemical composition of specimens nondestructively and with minimal sample preparation and handling. Optical spectroscopic techniques were recognized as such potential analytical tools and are increasingly being evaluated for their possible applications as probes of human disease and biological function. Diagnostic tests based on fluorescent labels of cellular metabolism[1] as well as fluorescence, infrared absorption, and Raman scattering from natural biomolecules[3] have been described as such analytical techniques.

Among these spectroscopic techniques, ultraviolet resonance Raman (UVRR) spectroscopy is being increasingly used to study biochemical processes in proteins, micro-organisms, cells, and tissues.[2,4–8] With tuning of the incident photon energy to the electronic energy level of the molecules under study, UVRR spectroscopy offers several advantages when compared to nonresonance Raman scattering. Increased Raman cross sections are achieved, and smaller concentrations of a given biochemical can be detected. Moreover, with tuning of the excitation wavelength to a particular molecule's absorption band, resonance Raman allows one to enhance the signal from specific scatterers and detect a specific compound in a complex mixture where many other compounds are present.

The advantages of UVRR spectroscopy are often counterbalanced by the complicated apparatus needed to generate the ultraviolet laser excitation and detect the ultraviolet Raman scattered radiation. However, recent improvements in laser design and photon detection technology have made UVRR easier to use, and applications to cells and whole tissue are emerging. In our laboratory, we have previously explored the use of UVRR spectroscopy to differentiate normal and diseased colon tissue, and the results showed the promise of UVRR to probe differences in nucleic acid content between normal and cancerous tissue.[2] In this report, we describe an improved UVRR system. Taking human colon mucosa as an example, we compare this new system to our previous Nd:YAG-based instrument for bulk tissue, and we use the present system to characterize spectroscopically the microscopic components that contribute to the UVRR spectrum of bulk human colon tissue.

EXPERIMENTAL

This section details the UVRR spectroscopy system for bulk and microscopic human tissue studies. An overall diagram of the setup is shown in Fig. 1. The bulk and microscopy systems use the same excitation source and spectrometer/detection apparatus, but they differ in their delivery/collection optics and sample holders.

Excitation Source. Our excitation source is similar to that of Doig and Pendergast[9] and uses the third or fourth harmonic of a tunable, mode-locked Ti:sapphire (Ti:Sa) laser pumped with an Ar^+ laser (Fig. 1). This quasi-continuous laser system produces 2–3 ps pulses at a 76 MHz repetition rate and is continuously tunable over the 200–300 nm range. The typical output power of the laser system is ~ 50 mW at 250 nm, ~ 10 m W at 240 nm, and ~ 1 mW at 230 nm.

Spectrometer/Detection System. The collected Raman scattered light is launched into a 1 m long $f/8$ spectrometer that disperses it at 0.4 nm/mm with a single 2400 grooves/mm grating across a liquid nitrogen-cooled charge-coupled device (CCD) detector. An entrance slit of 150 μm produces a spectrometer resolution of 0.06 nm (9 cm^{-1}), but the overall system resolution is limited to 15 cm^{-1} by the laser bandwidth. This resolution is

Received 25 March 1999; accepted 30 August 1999.

* Author to whom correspondence should be sent. Harvard-MIT Division of Health Sciences and Technology. Current address: Biomedical Engineering Department, Johns Hopkins School of Medicine, 720 Rutland Ave. Traylor 701, Baltimore, MD 21205.

0003-7028/00/5401-0024$2.00/0

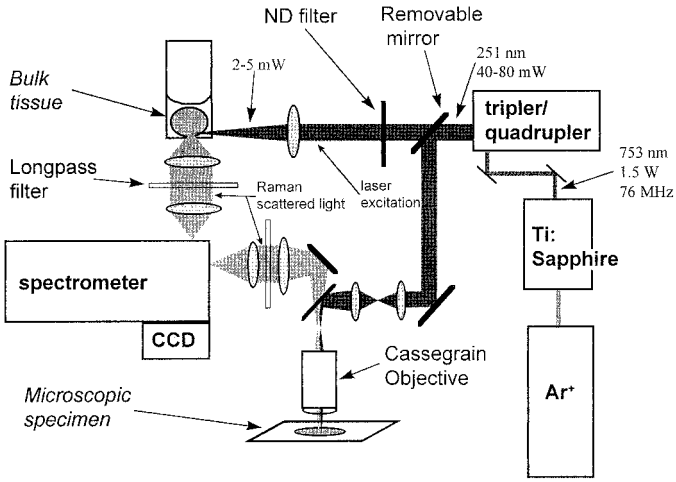

FIG. 1. Schematic diagram of the UVRR system. The excitation source is the third harmonic of a titanium : sapphire laser pumped by the multiple visible line output of an argon-ion laser. The ultraviolet light is directed either to a bulk tissue sample placed in a cuvette or to a microscopic specimen on a slide. The Raman scattered light from the samples is collected and focused on the entrance slit of a 1 m long spectrometer. The Raman light is dispersed by a single 2400 grooves/mm grating and detected by a liquid nitrogen-cooled CCD. A longpass filter is placed in the light collection path to reject Rayleigh scattered light at the laser excitation wavelength. Details of the bulk tissue and microscopy subsystems are shown in Fig. 3.

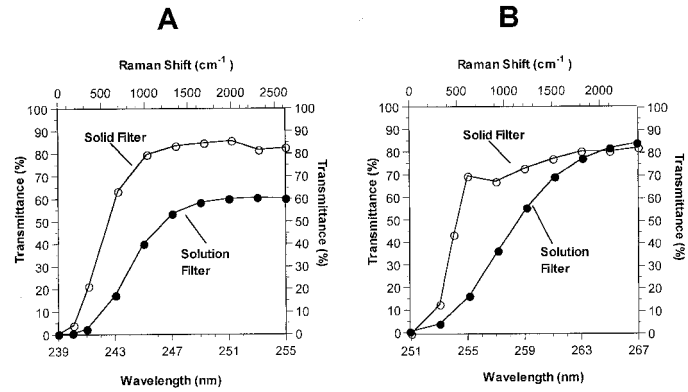

FIG. 2. Solid and solution longpass filter transmittance for 239 (**A**) and 251 (**B**) excitation. For 239 nm, the solution was 0.8×10^{-4} M quinoline dissolved in methanol. For 251 nm, a solution of 2.5×10^{-5} M anthracene, 0.5 M Potassium Iodide in ethanol : water (1:1::V:V), was diluted 13 times in pure ethanol. Both solutions were placed in a 1 cm pathlength quartz cuvette.

adequate for Raman studies of biological tissue, which has Raman bands approximately 30 cm^{-1} wide. Following standard procedures, the Raman shift axis of the CCD spectra was calibrated by a cubic fit[10] to known band positions of ethanol and acetone in the 1000 to 1800 cm^{-1} wavenumber range.[11,12] The spectra were not intensity calibrated since this calibration was not necessary for our studies where the Raman system was eventually used to compare relative changes between bulk and microscopic colon spectra.

Dielectric longpass filters (Barr Associates, Westford, MA) were used to reject the Rayleigh scattered light. These filters replaced the solution filters previously used by us and other investigators.[2,5,13] In Fig. 2, the transmittance of the solid filters is compared to that of the solution filters for 251 and 239 nm cutoff. For 239 nm, the solution was 0.8×10^{-4} M quinoline dissolved in methanol. For 251 nm, a solution of 2.5×10^{-5} M anthracene, 0.5 M potassium iodide in ethanol/water (1:1 v:v), was diluted 13 times in pure ethanol. Both solutions were placed in a 1 cm pathlength quartz cuvette. As shown in Fig. 2, in the range 1100–1800 cm^{-1} the new solid filters have a transmittance between 70 and 85%, which is greater than that of the solution filters. Also by transmitting wavelengths closer to the laser line, the solid filters expand the collection range down to ~ 500 cm^{-1}. For the solid filters, the transmittance at the laser wavelength is 0.32% for 239 nm and 0.25% for 251 nm; for the solutions filters 0.14% at 239 nm, and 0.53% at 251 nm. By adjusting the tilt angle of the solid filter with respect to the incoming light beam, one can achieve higher absorption at the laser wavelength with a small decrease in transmittance in the 1100–1800 cm^{-1} range. The solid filters also have a cut-off region between 400 and 500 nm (data not shown), which reduces background due to stray fluorescence. Other dielectric longpass filters were described by Pajcini et al.[7] and were manufactured by Omega Optical to reject 244 nm. Both in our case and in the work of Pajcini and colleagues, the filters were custom made.

Specimen Preparation and Set Up. *Bulk Specimens.* Samples of bulk human colon mucosa were obtained from patients immediately following partial colectomy. The samples were refrigerated and tested without freezing within 10 h of the resection, or snap frozen in liquid nitrogen and stored at −80 °C until later use. Normal colon mucosa samples were used to generate the bulk tissue spectra shown in this study. In the course of the study, bulk tissue samples were collected from six colon specimens of six patients. Two of these six specimens were frozen until later use. The samples that were frozen and thawed were only used for a period of up to 30 min after thawing. During spectroscopy, the bulk samples were placed in a cuvette with a calcium fluoride window, containing saline (pH = 7.4) and kept at 0–4 °C with thermo-electric coolers (Model CP 1.0-17-05L, Melcor Thermoelectrics, Trenton, NJ). Calcium fluoride was used instead of quartz to avoid the Raman bands of fused silica. The colon sample was positioned in the cuvette so that the mucosa faced the incident beam (Fig. 3A). To avoid collecting specular reflection of the laser light, the laser beam impinged on the cuvette surface at an angle of about 60° with respect to the optic axis, which is defined by the spectrometer. A neutral-density filter was placed in the excitation path to reduce the power striking the tissue to 2–5 mW. The Raman scattered light was collected along the direction perpendicular to the sample surface. The incident laser beam gave a rectangular spot area 35 by 40 μm.†

The tissue sample holder was mounted on a translational stage, and the stage actuator was connected to a 4 rpm ac motor to move the sample across the incident beam at about 2 mm/min. This movement minimized laser exposure time on an individual spot (about 1.5 s/spot).

† The incident laser beam had a rectangular cross section, 0.5×1 cm^2, and was estimated to give a 10×20 μm^2 diffraction-limited spot after focusing with a 15 cm focal length lens.

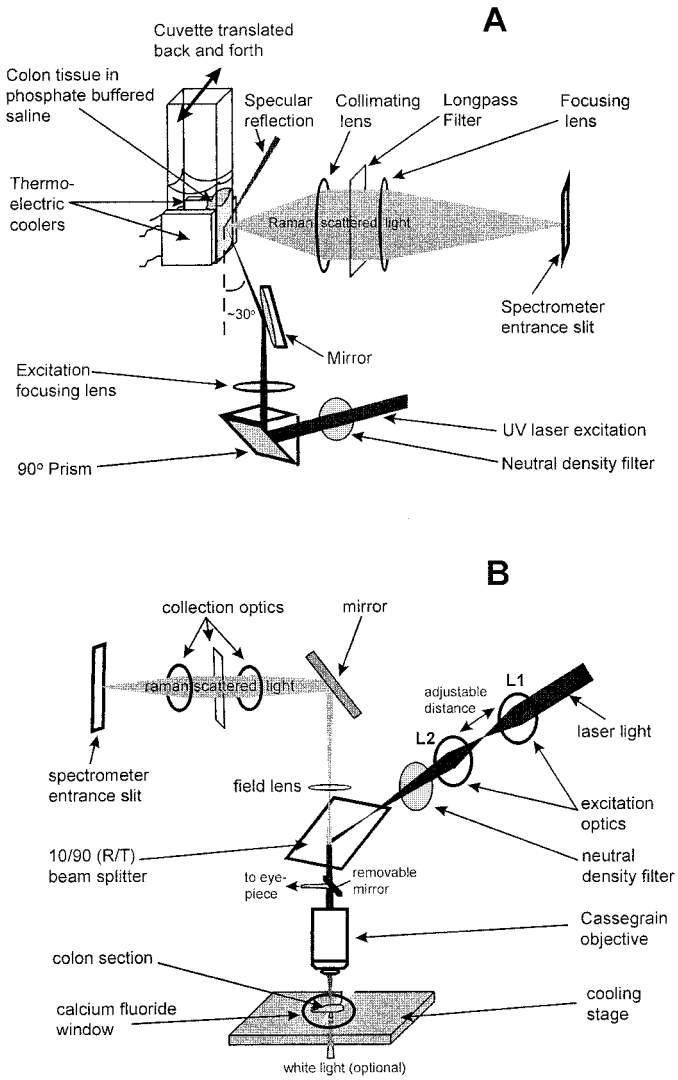

FIG. 3. (**A**) Detail of the bulk tissue system. Human colon specimens obtained after surgical resection are placed with the mucosa facing the incident laser beam in a cuvette with a calcium fluoride window, partially filled with phosphate buffered saline (pH = 7.4). The cuvette and saline are cooled to 0–4 °C by 2 thermo-electric coolers. Ultraviolet light excites the sample by impinging on the calcium fluoride surface at an angle of about 60° with respect to the collection axis. The Raman scattered light is collected along the direction perpendicular to the sample surface. The cuvette is translated during data acquisition to minimize photodamage by minimizing laser exposure time on an individual spot. The laser spot size was 35 by 40 μm. (**B**) Detail of the microscopy system. Frozen sections of human colon mucosa are mounted on a calcium fluoride window and kept at 0–4 °C by placing the window on a cooled stage. The ultraviolet laser radiation and the Raman scattered light are coupled to the tissue section by the same Cassegrain objective. A beamsplitter positioned above the objective reflects 10% of the laser light and transmits 90% of the Raman scattered light. A removable mirror is used to direct the sample's white light image to the eye-piece for specimen visualization during sample positioning and focusing. The mirror is removed during spectroscopy. The laser is focused on the sample by adjusting the distance between the two lenses L1 and L2. The laser spot size was 20 μm^2.

A 3.3 mm strip along the tissue surface was scanned by the laser during a typical signal collection time of 100 s.

Microscopic Specimens. For microscopy, frozen colon sections were obtained from the bulk colon specimens collected after surgery, previously snap frozen in liquid nitrogen, and stored at −80 °C. Frozen bulk tissue was mounted without thawing on standard mounting medium (Histo Prep, Fischer Scientific, Fair Lawn, NJ). The mounting medium with the tissue in place was frozen in liquid nitrogen. The tissue fixture thus obtained was placed in a microtome, and the tissue was cut into 24 μm thick sections. The microscopy frozen sections were placed on ice-cold calcium fluoride substrates immediately after slicing and transported on ice to a microscope stage cooled to 0–4 °C (Physitemp, Clifton NJ) for spectroscopic examination. Each section was tested for only up to 30 min after cutting. Typically, tissue specimens were stationary during microscopic examination, as opposed to the bulk system, in which the specimens were translated during signal collection. Individual spectra were collected in 10 s.

The microscopy system is depicted in Fig. 3B. The UV excitation light was shaped by two lenses (L1 and L2), redirected with a beamsplitter, and focused onto the sample with a Cassegrain microscope objective. Scattered light was collected by the same objective and then directed and focused onto the spectrometer entrance slit by a mirror, a collimating lens, and a focusing lens. A calcium fluoride field lens between the objective and the mirror was used to increase light collection. A neutral-density filter was placed in the excitation light path to control sample illumination power to 0.1–0.3 mW. The microscope body was by Olympus (Melville, NY).

The sample was positioned into the microscope focus by looking at the sample under white light through the microscope eyepiece. Then, the laser light was focused onto the sample, without moving the microscope stage, by changing the separation between lenses L1 and L2. The beamsplitter, a quartz plate that is anti-reflection (AR) coated on the side opposite the laser beam (custom-made plate, CVI, Putnam, CT), reflected 10% of the *s*-polarized laser light and transmitted 90% of the collected scattered light. The excitation optics were designed to optically fill the objective lens with the incident laser beam to minimize the excitation spot size on the sample. This spot size determined the microscope spatial resolution. The 15× reflecting objective (Ealing Electro-optics, Holliston, MA, Model 25-0506) used in this study yielded a spot diameter of 5 μm. The depth of field was measured to be between 75 and 100 μm.

Microscopic data acquisition consisted of collecting spectra from the different morphological tissue components of colon. Spectra were acquired from normal crypt cells (42 spectra), lamina propria (45 spectra), submucosal extracellular matrix (36 spectra), and lipid (2 spectra). Given the 24 μm section thickness and the 20 μm^2 spot size, each cell spectrum comes from portions of two adjacent cells (a cell being approximately 20 μm thick). For each component, data were collected from a few non-adjacent sections. When spectra were collected from crypt cells, the sections were sliced parallel to the mucosal surface (*en face*). Lipid was scanned from the perivascular fatty regions around capillaries in the submucosa. The lipid spectra were collected from the same section. Sequential acquisitions were collected to ensure that no spectral changes occurred during the acquisition period. At least two consecutive unchanged spectra were collected for each point.

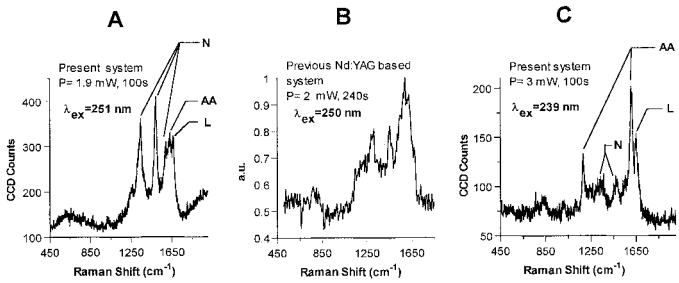

FIG. 4. Representative spectra from normal bulk colon tissue at 251 and 239 nm. Colon samples were harvested from patients immediately after partial colectomy. All three spectra in this figure were acquired from samples that were snap frozen in liquid nitrogen upon collection, and stored at −80 °C until use. The spectra in panels **A** and **C** were from the same patient. Ultraviolet resonance Raman spectra of colon show contributions from nucleotides (N at 1337, 1485, and 1585 cm^{-1}), the aromatic amino acids tryptophan and tyrosine (AA at 1620 cm^{-1} and at 1174 cm^{-1} for 239 nm) and lipids (L at 1650 cm^{-1}). At 251 nm (**A**), nucleotide bands dominate the spectrum, while amino acid bands dominate the spectrum at 239 nm (**C**). The signal-to-noise ratio in the spectra is approximately 30:1 at 251 nm and 20:1 at 239 nm, and the baseline is due to background light primarily from undispersed visible fluorescence. In panel **B,** a spectrum of normal colon acquired previously in our laboratory[2] with 250 nm excitation is shown for comparison with the present system. Accounting for the differences in incident energy, the present system outperforms the previous Nd:YAG-based system with an improved signal-to-noise ratio by a factor of more than 10 (compare nucleic acid bands at 1337 cm^{-1} and 1485 cm^{-1} in panels **A** and **B**).

RESULTS AND DISCUSSION

The spectra presented in this section were not smoothed, (except for Fig. 5B). Spectral spikes due to cosmic rays were subtracted by using an algorithm designed in our laboratory.‡

Bulk System Performance. Typical colon spectra collected with 251 and 239 nm wavelength excitation are shown in Fig. 4. The spectra were collected from frozen samples and show contributions from nucleotides (N), amino acids (AA), and lipids (L). At 251 nm excitation (Fig. 4A) the major nucleotide bands are due to pyrimidine and imidazole ring vibrations,[14] the amino acid bands are due to the benzene ring vibration from tyrosine and tryptophan,[15] and the lipid band is due to the C=C vibration.[2] This last band was an artifact resulting from undissolved lipid in the saline covering the tissue. This lipid is derived from the fatty tissue attached to the serosal side of the bulk colon specimen. The incident power on the sample was 1.9 mW at 251 nm, and the collection time was 100 s. This approach produced a signal-to-noise ratio (S/N) of 30:1.

At 251 nm, the spectrum is dominated by the features of the nucleotides, which have absorption bands near 260 nm. In contrast, the colon spectrum with 239 nm excitation is dominated by aromatic amino acid bands near 1620 cm^{-1} (Fig. 4C). The 239 nm excitation is closer to the aromatic amino acid absorption around 220 nm. With 3 mW of power and 100 s acquisition time, the S/N was 20:1 at 239 nm. The spectra in Figs. 4A and 4C illustrate how selective Raman cross-section enhancement can be achieved by tuning the excitation wavelength to an absorption band of the molecules under study. The baseline background in Figs. 4A and 4C is caused primarily by undispersed stray light originating from sample fluorescence. This background was minimized by placing a mask inside the spectrometer in front of the CCD to deflect stray light.

The 251 nm colon spectrum was compared with a spectrum from normal colon collected with the Nd:YAG-based system.[2] That previous system used stimulated anti-Stokes Raman lines of the fourth harmonic of a Nd:YAG laser as an excitation source, and a multichannel analyzer for signal collection. Due to the improvement in the efficiency of the detection/collection apparatus, the current system has an S/N more than 10 times greater than the previous system (compare Fig. 4A with 4B). The line shapes in Figs. 4A and 4B are also qualitatively different, with a much lower nucleotide signal compared to amino acids in Fig. 4B. Separate experiments[16] have shown that photobleaching and biochemical degradation result in a spectral change manifested by a decrease in the adenyl and guanyl UVRR scattering signals (signals at 1337 and 1485 cm^{-1}). We have extensively investigated the rate of photobleaching as a function of laser fluence and temperature, and have shown that the rate of photobleaching was significantly decreased when the sample was kept at ~4 °C compared with room temperature. Biochemical degradation due to freezing and thawing, independently of laser exposure, was also found to corrupt our spectra by causing a specific decrease in the adenyl signal, and sample freshness was prolonged by conducting our spectroscopy in a refrigerated setup. Thus, in a procedure to minimize both biochemical degradation and photobleaching, sample coolers were incorporated into the present bulk and microscopy systems. Artifacts due to any one of these two degradation effects may account for the difference in line shapes observed when comparing our present spectra (Fig. 4A) with those acquired from our previous UVRR system (Fig. 4B).

Microscopy System Performance. A spectrum of a crypt cell area in a 24 μm-thick section of colon mucosa is shown in Fig. 5. This spectrum was collected in 10 s with approximately 0.3 mW of 251 nm excitation light. The signal-to-noise ratio in the raw spectrum (Fig. 5A) is 5:1. A smoothed version of the same spectrum is shown in Fig. 5B to enhance the spectral line shape, which is dominated by nucleotide Raman bands. Since the microscopic spectra were acquired from a stationary spot on the specimen, the collection time period, and therefore S/N, was limited by photobleaching. To acquire spectra with a minimal amount of photobleaching artifacts (signal less than 5% photobleached), we found that the maximum fluence that could be used was 0.2 mJ/μm^2.[16] In addition to the background noise due to fluorescence stray light as in the bulk system spectra, noise in the microscopy system is due to an increase of Rayleigh scattered light entering the spectrometer. The amount of Rayleigh scattered light contributing to the background was 36 times larger in the microscope than in the bulk system, due to specular reflection of the laser

‡ Briefly, the algorithm consisted of scanning the spectrum and comparing the intensity of every point to the average intensity of a region spanning ±8 pixels around that point. If the intensity at that center point was 3× the standard deviation of the mean within the given 16 pixel window, the intensity at that center point was made equal to the average intensity in the window. Each spectrum spanned 1035 pixels between 450 and 2000 cm^{-1}.

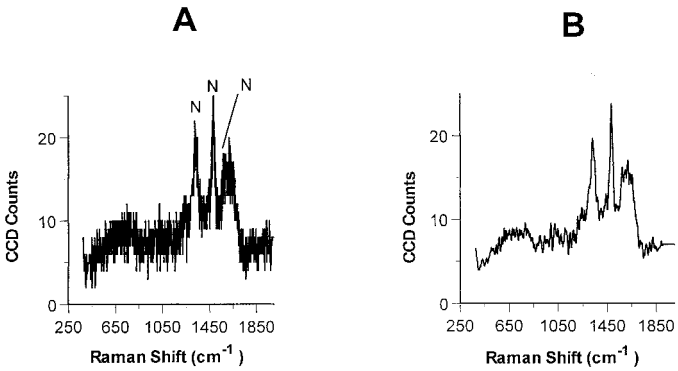

FIG. 5. Raw (**A**) and smoothed (**B**) UVRR spectrum of colon crypt cell area collected at 251 nm. This spectrum was collected from a 24 μm thick frozen section of human colon mucosa. The excitation region was 5 μm in diameter. This spectrum included one or two crypt cells. The incident power on the sample was approximately 0.3 mW and the collection time was 10 s. Under these conditions, this spectrum is less than 5% photobleached. Nucleotide bands (N) dominate this spectrum with a signal-to-noise ratio of 5:1 in the raw data case (**A**). In an effort to enhance the spectral line shape, the spectrum in **A** was smoothed (panel **B**) by using the digital smoothing polynomial technique (Savitsky–Golay smoothing).[17]

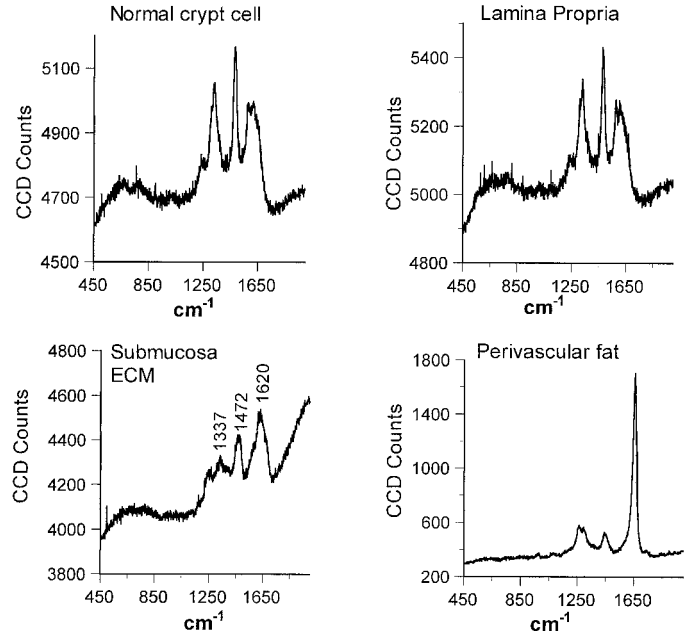

FIG. 6. Line shapes of the microscopic morphological components of normal colon tissue collected at 251 nm excitation. Average line shapes of the different microscopic structures were generated as described in the specimen preparation and setup section. These spectra represent the sum of spectra collected from many spots in a given compartment. For the average cell spectrum, we added 42 × 10 s spectra, for the lamina propria 45 × 10 s spectra, and for the ECM 36 × 10 s spectra. For the perivascular fat, the spectrum is the sum of one spectrum collected with 2.5 mW for 10 s and one collected with 0.3 mW for 100 s. Except where noted, the power was approximately 0.3 mW for each individual spectrum and the spot size was 20 μm^2.

light from the sample and into the microscope collection optics.

Other UVRR microscopy systems, which use 257 or 244 nm excitation light, have been described.[4–7] In particular, Nelson, Chadha, and Sureau et al. directed the UV excitation light to the sample with an external set of optics without launching the beam into the microscope objective.[4–6] This configuration minimizes collection of specular reflection and should result in a significant decrease in Rayleigh scattering background. This external laser excitation configuration is also advantageous for controlling the intensity of the light striking the sample. In an arrangement to minimize the intensity of the potentially photodamaging UV light that strikes the sample, the laser beam in Sureau's system was focused onto a 100 μm^2 area on the sample, and an aperture in the collection optics was used to select a 20 μm^2 area to be studied. However, the external excitation technique makes it difficult to control where the laser light strikes the sample. As the microscope stage is raised or lowered to bring the sample into focus, the laser light moves across the sample and thereby translates the area under study. Recently, a UVRR microspectroscopy system with 244 nm excitation was described by Pajcini et al.[7] In this system the laser excitation is focused on the sample via a prism mounted under a Cassegrain objective. The laser light impinges perpendicularly on the sample surface. This configuration blocks the specular reflection from the sample and therefore should significantly reduce the Rayleigh scattering background. One disadvantage of this system is that the excitation spot size, which limits the lateral resolution of the system, is no longer as small as could have been achieved by epi-illumination through the microscope objective.

Microscopic UVRR Study of Colon Tissue Structure. The present UVRR system was used to spectroscopically describe a histological section, and spectra of the different microscopic components of colon tissue were generated. Figure 6 shows the average spectra of the different microscopic tissue components: cells, lamina propria, extracellular matrix, and perivascular fat. For each component, a number of individual spectra collected from different individual spots were summed (see "Microscopy Specimens"). For the cells, lamina propria, and submucosa, the laser power at the sample was 0.275, 0.25, and 0.325 mW, respectively, and the acquisition time was 10 s per individual spectrum. For the first lipid spectrum, the power was 2.5 mW and the acquisition was 10 s. For the second lipid spectrum, the power was 0.3 mW with a 100 s acquisition (longer collection times could be used in this case since perivascular fat was much less susceptible to photobleaching than other morphological component). The spot size in all cases was 20 μm^2.

In Fig. 6, the cell average spectrum has a strong nucleotide contribution at 1337, 1485, and 1585 cm^{-1}. The average spectrum of lamina propria is very similar to that of a normal cell. This result is due to the fact that a large amount of leukocytes in the lamina propria is sampled in the 24 μm section. The average spectrum of submucosal extracellular matrix (ECM) mainly consists of the protein contribution around 1620 cm^{-1}. The ECM spectrum is similar to that of collagen (Fig. 7). However, the ECM peak centered at 1472 cm^{-1} is broader than that of collagen (at 1463 cm^{-1}), possibly due to a nucleotide contribution at 1485 cm^{-1}. These nucleotides may come from the cells present in the submucosa and may also contribute to the small signal observed at 1337 cm^{-1} in the ECM spectrum. The spectrum of perivascular fat mainly consists of the C=C vibration at 1650 cm^{-1}. These spectra

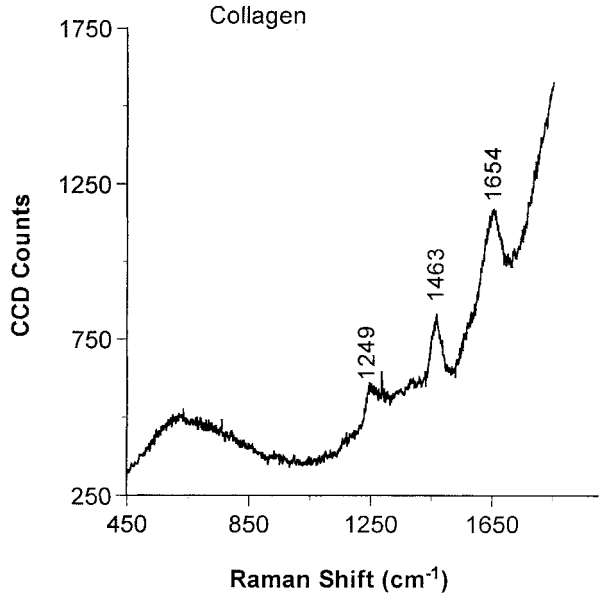

FIG. 7. UVRR spectrum of collagen at 251 nm excitation. This spectrum was collected from a collagen gel made by partially dissolving collagen type III (from calf skin, Sigma, St. Louis, MO). The spectrum was collected while translating the sample in the bulk UVRR system. The power on the sample was 2.5 mW. The spot size was 35 μm × 40 μm, the translation rate was 2 mm/min, and the acquisition time was 100 s.

show how UVRR microscopy could provide spatial distribution of biochemicals within a histological section.

The microscopic spectra were compared to the bulk tissue spectra to infer which morphological tissue components contribute to the bulk tissue spectrum. By comparing Figs. 6 and 4A, we find that the main contributors to the bulk colon spectrum are the crypt cells and the lamina propria, which have a significant nucleotide content. This finding is consistent with the 30 μm sampling depth of ultraviolet light in colon at 251 nm, measured in a separate study.[16] Given that the epithelial thickness in colon mucosa is 35 μm,[18,19] the measured sampling depth implies that approximately 70% of the Raman scattered light originates in the epithelial layer, while the remaining 30% originates from the 70 μm of underlying tissue, in this case the lamina propria. The submucosa, which starts 400 μm below the tissue surface, does not contribute to the bulk tissue signal.

CONCLUSION

We have built a state-of-the-art UVRR system well suited for studying bulk and microscopic human tissue. By improving our laser source and our Raman collection setup including the use of new solid rejection filters and sample cooling, we have greatly increased our ability to collect spectra from human tissue with larger signal-to-noise ratio than has been previously achieved. Our data suggest that combined bulk and microscopic UVRR spectroscopy could provide a valuable tool for biochemical and morphological analysis of human tissue, with the potential for significant applications in histopathology and histochemistry.

In this paper, we have used UVRR microspectroscopy to assess which morphological components contribute to the spectra of bulk colon tissue. One potential application of using UVRR spectroscopy in this manner is to reconstruct the bulk tissue spectrum from the individual tissue microscopic components. Ultimately, a quantitative analysis analogous to morphometry could be implemented, whereby the bulk tissue spectrum could, for example, be modeled as a linear combination of the individual microscopic components in a least-squares minimization. The relative contribution of each morphological compartment can then be calculated and correlated with the actual tissue composition.

The possibility of using UVRR spectroscopy for cytological screening of cells in suspension has been recently discussed by Yazdi et al.[8] In addition, the ability to collect UVRR spectra from microscopic tissue sections should have significant applications in histopathology and histochemistry. In histopathology, which typically provides morphological information, specific biochemical information can be obtained with the use of special staining techniques, such as immunostaining and fluorescence. UVRR spectroscopy could complement these existing techniques by providing biochemical information nondestructively, without extensive sample preparation, as is usually the case prior to staining. UVRR spectroscopy of the colon epithelium with 251 nm excitation directly provides information on nucleotide content relative to amino-acid content with minimal sample handling. One possible application of this could be "microscopic cell sorting", where tissue sections could be analyzed with UVRR spectroscopy to detect aneuploid cells with higher levels of nucleic acid for instance. In contrast to fluorescence-based flow cytometry, UVRR spectroscopy can be used to sort cells within a given microscopic section without destroying them, thus allowing further bioassay of the same sample. With improved sensitivity, UVRR monitoring of live cells subjected to different experimental conditions, such as drug screening protocols, may become possible. Nondestructive biochemical assays of microscopic specimens may have important uses in biotechnology, and UVRR spectroscopy may provide one such technique.

ACKNOWLEDGMENTS

We thank Dr. James Crawford who provided the human colon samples used in this study. This work was conducted at the MIT Laser Biomedical Research Center and supported by NIH Grant No. P41-RR02594. Additional support for equipment and research was also provided by NIH Grant No. Ro1-CA53717 and NSF Grant No. 9304251.

1. W. T. Mason, "Confocal Raman Microspectroscopy", in *Fluorescent and Luminescent Probes for Biological Activity, A Practical Guide to Technology for Quantitative Real-time Analysis* (Academic Press, San Diego California, 1993).
2. R. Manoharan, Y. Wang, R. R. Dasari, S. S. Singer, R. P. Rava, and M. S. Feld, Lasers Life Sci. **6,** 1 (1994).
3. R. Richards-Kortum and E. Sevick-Muraca Annu. Rev. Phys. Chem. **47,** 555 (1996).
4. F. Sureau, L. Chinsky, C. Amirand, J. P. Ballini, M. Dusquesne, A. Laigle, P. Y. Turpin, and P. Vigny, Appl. Spectrosc. **44,** 1047 (1990).
5. W. H. Nelson, R. Manoharan, and J. F. Sperry, Appl. Spectrosc. Rev. **27,** 67 (1992).
6. S. Chadha and W. H. Nelson, Rev. Sci. Instrum. **64,** 3088 (1993).
7. V. Pajcini, C. H. Munro, R. W. Bormett, R. E. Witkowski, and S. A. Asher, Appl. Spectrosc. **51,** 81 (1997).
8. Y. Yazdi, N. Ramanujam, R. Lotan, Mitchell M. Follen, W. Hittelman, and R. Richards-Kortum, Appl. Spectrosc. **53,** 82 (1999).

9. S. J. Doig and F. G. Prendergast, Appl. Spectrosc. **49,** 247 (1995).
10. S. T. Wollman and P. W. Bohn, Appl. Spectrosc. **47,** 125 (1993).
11. D. Strommen and K. Nakamoto, *Laboratory Raman Spectroscopy* (John Wiley and Sons, New York, 1984), pp. 115, 118.
12. G. Dellepiane and J. Overend, Spectrochim. Acta **22,** 593 (1966).
13. E. Ghiamati, R. Manoharan, W. H. Nelson, and J. F. Sperry, Appl. Spectrosc. **46,** 357 (1992).
14. S. P. A. Fodor, R. P. Rava, T. R. Hays, and T. G. Spiro, J. Am. Chem. Soc. **107,** 1520 (1985).
15. B. S. Hudson and L. C. Mayne, ''Peptides and Protein Side Chains'', in *Biological Applications of Raman Spectroscopy,* Vol. 2, T. G. Spiro Ed. (Wiley Interscience, New York, 1987).
16. N. Boustany, Ph.D. Thesis, Harvard-M.I.T. Division of Health Sciences and Technology, Cambridge, Massachusetts (1997).
17. W. H. Press, S. A. Teulosky, W. T. Vetterling, and B. P. Flannery, *Numerical Recipes in C. The Art of Scientific Computing* (Cambridge University Press, New York, 1992), 2nd ed.
18. M. V. Grondin, W. W. L. Chang, R. D. Gaskins, Dig. Dis. Sci. **35,** 12 (1990).
19. T. J. Eide, Virchows Arch. A, **410,** 119 (1986).